Groundwater flow through continuous permafrost along geological boundary revealed by electrical resistivity tomography

Mikkel Toft Hornum[1,2], Peter Betlem[1,3], and Andy Hodson[1,4]

[1]Department of Arctic Geology, The University Centre in Svalbard, N-9171 Longyearbyen, Svalbard, Norway, [2]Department of Geosciences and Natural Resource Management, and Center for Permafrost, University of Copenhagen, 1350 Copenhagen K, Denmark, [3]Department of Geosciences, University of Oslo, Sem Sælands Vei 1, N-0371 Oslo, Norway, [4]Department of Environmental Science, Western Norway University of Applied Sciences, Røyrgata 6, N-6856 Sogndal, Norway.

Corresponding author: Mikkel Toft Hornum (mth@ign.ku.dk)

Contents of this file

Additional Supporting Information (Files uploaded separately)

Text S1. Quality check and pre-processing of measured ERT data

Prior to the inverse modelling of the measured electrical resistivities with ResIPy 3.0.0 (Blanchy et al., 2020), we performed quality checks and data cleaning to ensure a more accurate final resistivity image. During the field experiments, measured resistivity data was stored on the device (ABEM SAS-1000 Terrameter) in a binary file format (.SK4). Using the instrument specific software Terrameter SAS4000/SAS1000 Utilities (Guideline Geo AB, Stockholm), data files was retrieved from the instrument and converted to ASCII text files. In accordance with the desired input for ResIPy, the final product of the pre-processing was four files, one for each Transect, containing the unique electrode configurations and one transfer resistance value for each of these configurations (i.e., 'protocol.dat'-format; Binley, 2019). Whenever several measurements were available for the same electrode configuration (data point), we chose the statistically most significant ones and used the mean as input for the inverse modelling. Table S1 provides a numeric overview of the pre-processing and data cleaning, while a description is given in the following.

<u>Merging of files and removal of non-reciprocal measurements</u>

Measurements from the same run-along profile were merged into one file and the electrode numbers corrected accordingly. Empty measurements and measurements with no reciprocity were discarded leaving only complete measurements pairs (i.e., a normal and its reciprocal measurement). Prior to further data cleaning and pre-processing, the amount of complete measurements pairs prior comprised between 87–95% of the measurements scheduled in the recording protocol (Table S1).

<u>Removal of measurements with high error (normal vs. reciprocal measurements)</u>

The transfer resistance misfit was calculated for each measurement pair, and those with errors greater than 5% were discarded. Of the remaining measurement pairs, those with errors greater than three standard deviations were also removed (Figure S1). After the removal of these measurements, 83–91% of the scheduled measurements remained. The location of unique data points and the number of measurements pairs for each of these are plotted on Figure S2, which shows that 87–93 % of the unique data points scheduled in the measurement protocol were covered after the removal of measurements with high error. Root-mean-square errors (RMSE) of the remaining measurement pairs between 0.4–1.2% quantifies the data quality (Figure S1).

<u>Final data cleaning</u>

The final data cleaning was based on the mean of transfer resistances of each remaining measurement pair.
Despite a relatively good agreement between normal and reciprocal measurements (as indicated by the RMSEs, Figure S1), measurement pairs from the same data point did not always agree. This is exemplified on Figure S3, which shows transfer resistances measured with the minimum electrode spacing at Transect A. From this Figure, it is obvious that some measurements deviated by showing significantly higher transfer resistance values than the remainder. These were not regarded to represent true ground conditions, and called for further data cleaning. In order to meet with this call, we consecutively performed the data cleaning steps described below.

- By plotting all measurements like on Figure S3 (not shown), we could visually infer a transfer resistance threshold of 20 Ω and discarded all measurements above this

value. The only exception was for Transect C, were the threshold was defined by a transfer resistance of 27 Ω. The upper panels (a and c) of Figure S4 exemplify transfer resistances that remain after discarding those above the threshold. Further data cleaning, as described below and exemplified by Figure S5, were carried out on these measurements and resulted in the cleaned dataset, which is exemplified by the transfer resistances plotted on the lower panels (b and d) of Figure S4.

- For data points with four measurement pairs remaining, we discarded any measurements if outside the standard deviation. As exemplified by Figure S5a, this resulted in zero, one or two measurement pairs being discarded (subplot 2, 3 and 1, respectively).
- For data points with three measurement pairs remaining, we removed the most outlying measurement pair, but only if the difference to the median was more than twice the difference between the median and the third measurement pair. Thus, on subplot 1 of Figure S5b, the upper measurement pair was discarded; while on subplot 2, no measurements were discarded.
- For data points with two measurement pairs, we used a running mean, $\tilde{\mu}_n$, calculated from the mean, μ_n, of measurements a the data point, n, and the four neighboring data points at the same recording depths (n-2, n-1, n+1, and n+2). As exemplified by subplot 3 on Figure S5c, no measurements were discarded when $\tilde{\mu}_n$ was greater or smaller than both measurement pairs. When $\tilde{\mu}_n$ was between the measured transfer resistances, the measurement pair with the largest difference to $\tilde{\mu}_n$ was discarded, but only if the difference between μ_n and $\tilde{\mu}_n$ was greater than the difference between $\tilde{\mu}_n$ and the second measurement pair. Thus, on subplot 1 of Figure S5c, the measurement pair with the highest transfer resistance was discarded; whereas no measurements on subplot 2 were discarded.
- Finally, for data points with only one measurement pair, we discarded it, if the difference to the aforementioned running mean was greater than 3 Ω. This is exemplified by Figure S5d were two measurement pairs show transfer resistances that deviate more than 3 Ω from the running mean.

Text S2. Reliability of resistivity models

In this supporting text, we consider the reliability of the electrical resistivity values predicted by the resistivity models (Figure 4) by evaluating the sensitivity maps. Indicating good constrain for the inversion, log-sensitivity values above zero dominated the majority of the resistivity models and suggests that most of the predicted values represent true ground conditions. When low resistivity values dominate shallow ground conditions, the depth of current flow is reduced and measurements are thus less sensitive to deeper layers of the subsurface (Binley, 2015). This is reflected in the low sensitivity values for Segment III and the resistivity values predicted deeper than the shallowest couple of meters should thus be considered as tentative.

The shallow low resistivities imply that Segment III (Figure 4) may conceal zones of higher resistivities at greater depth. To quantify this potential concealment, we conducted a series of forward modelling experiments with ResIPy, which are described in the following. The fine mesh domain was 50 x 700 m and the mesh was defined using the same setup as for the inversion of the field measurements (Section 3). The starting (target) resistivity model consisted of two layers: a shallow layer with a low resistivity of 5 Ωm that was intended to mimic the shallow subsurface conditions of Segment III; and a deeper layer with a high

resistivity of 100, 500, 1000 or 2000 Ωm. The boundary between the two layers was located at a depth of 5, 10, 15, 25 or 35 m. The synthetic measurement protocol was defined as for the field measurements (i.e. 10 m electrode spacing, Wenner-α setup and mimicking roll-along layout) resulting in 605 unique electrode configurations (similar to Transect A and D but without topography, Figure S2). Given the starting resistivity models, domain setup and measurement protocol, the forward models could be run. Two percent noise was added to the synthetic measurements to simulate scenarios that are more realistic. The synthetic measurements were then inverted—again, using the same setup as for the field measurements.

Figure S6 shows the resistivity models produced by the forward modelling experiments, and a black dashed line is drawn to indicate which scenarios are compatible with the resistivity values predicted on Segment III (Figure 4) and which are not. The experiments suggests that if ground resistivities of 500 Ωm or more are situated above 15 m b.g.l., a survey design like the one employed here would predict resistivity values higher than what is observed in Segment III. Therefore, while the low sensitivity of Segment III does not allow for a detailed interpretation of the subsurface conditions, the predicted values still show that low resistivities dominate at least the shallowest 15 m b.g.l. and likely extent to more than 25 m b.g.l.
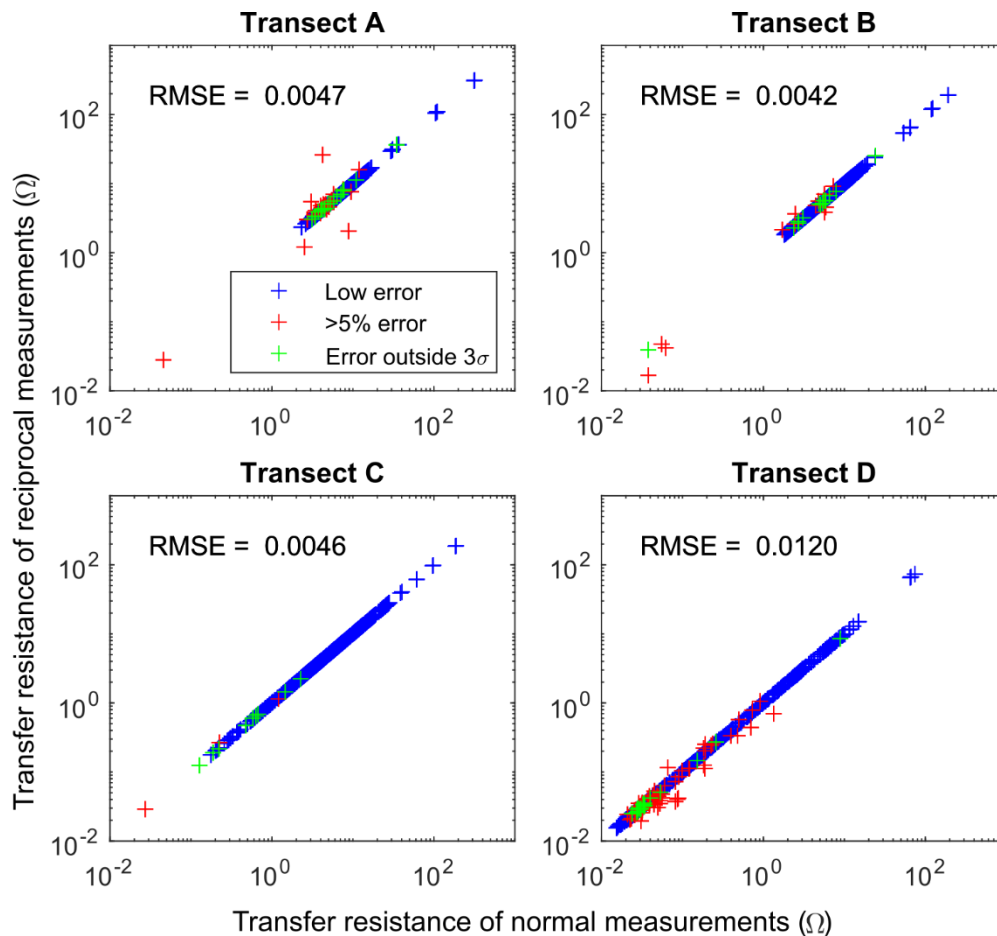

Figure S1. Transfer resistances of normal and reciprocal measurements. Measurement pairs with more than 5% error and errors outside three standard deviations (σ) were discarded. The root-mean-square errors (RMSE) are of the remaining measurements with relatively low error.
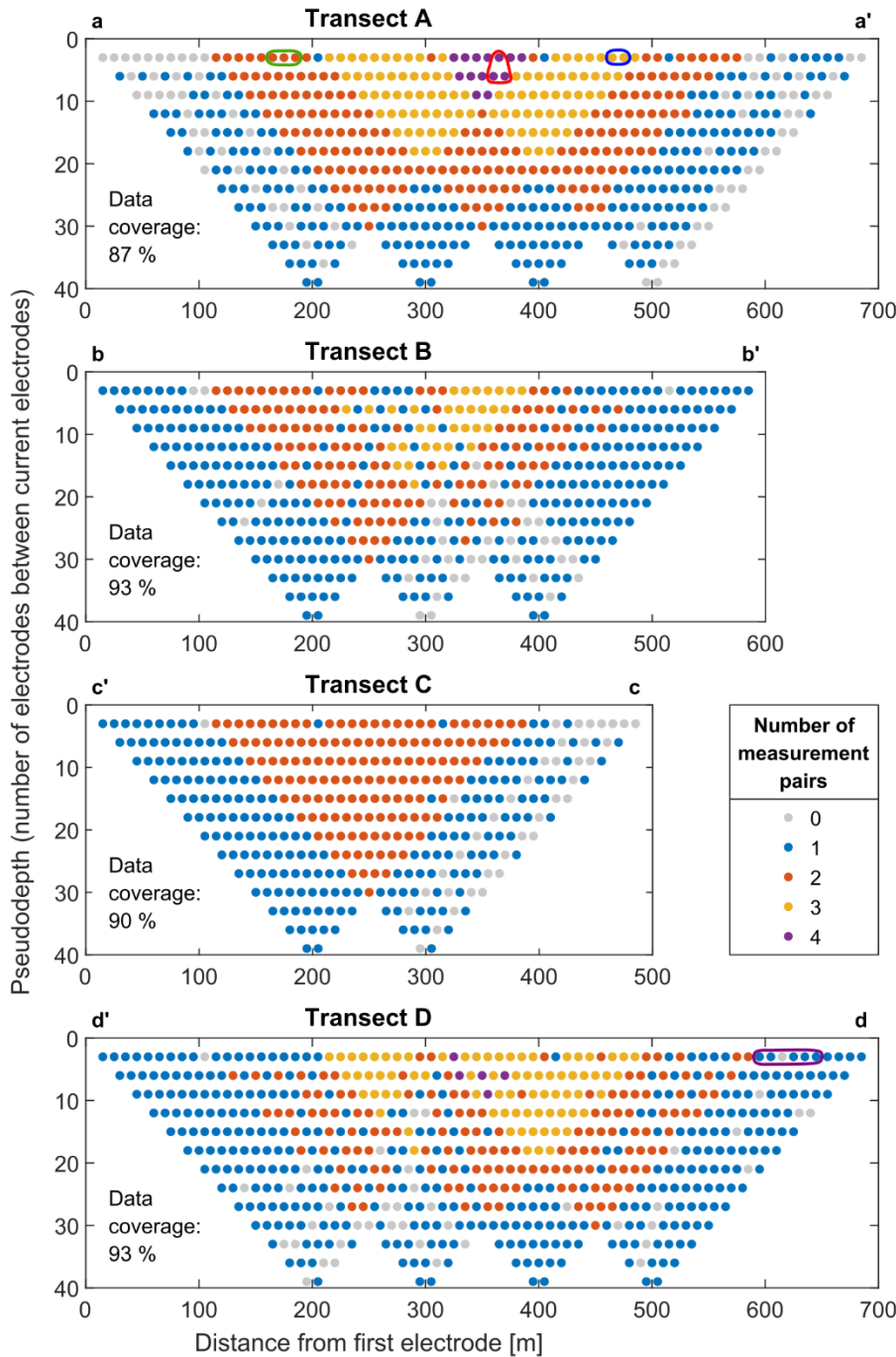
Figure S2. Overview of unique data points and number of measurement pairs remaining after removal of measurements with high error (Figure S1). Each data point correspond to a unique electrode configuration and its color indicates the number of complete measurements pairs recorded during the survey. The data coverage (lower left corner of each panel) indicates the proportion of unique data points with low error measurement pairs. Bold lowercase letters at the top of each transect indicate its orientation (see insert on Figure 3, main text). The data

points surrounded by a red, blue, green or purple line are used as examples for data cleaning on Figure S5.
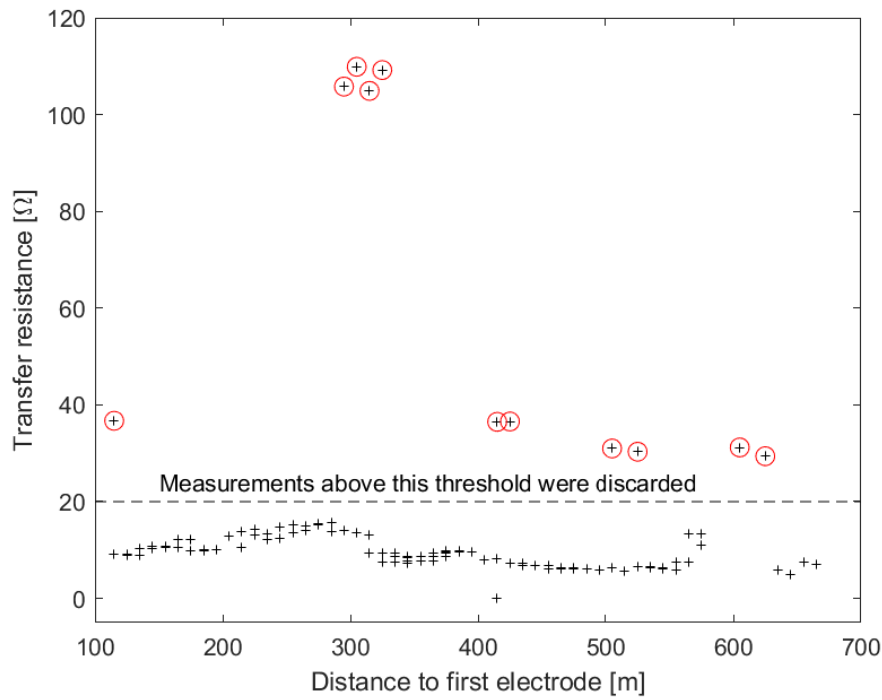
Figure S3. Transfer resistances measured with the minimum electrode spacing at Transect A. Each data point corresponds to the mean of a measurement pair. Red circles show that some measurements deviated by a considerably higher transfer resistance than the remainder. We discarded these by defining a visually interpreted upper threshold of 20Ω. Only measurement pairs with low error are included (colored data points on Figure S2).
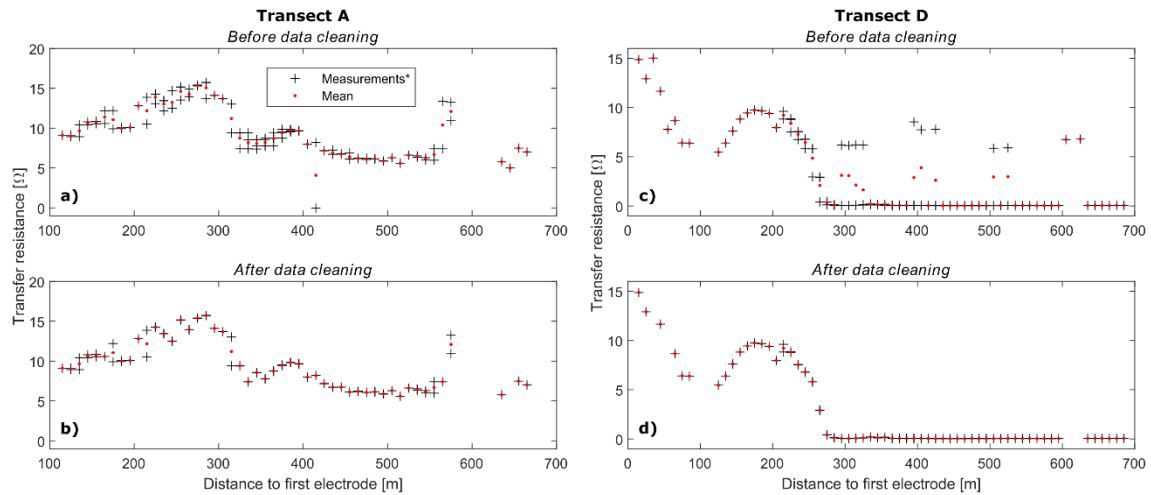

Figure S4. Transfer resistances measured with the minimum electrode spacing at Transect A (**a** and **b**) and D (**c** and **d**) before and after the final data cleaning. The upper panels, **a**) and **c**), show all measurements* that remain after the measurements above the threshold has been

discarded (Figure S3). The lower panels, **b**) and **d**), show the measurements* that remain after the final data cleaning. *Black crosses correspond to the mean of a measurement pair. The mean of measurements from the same data point (i.e. same distance on the x-axis) are drawn with red dots. The red dots in the lower panels (**b** and **d**) represent the transfer resistance values used for the inverse modelling.
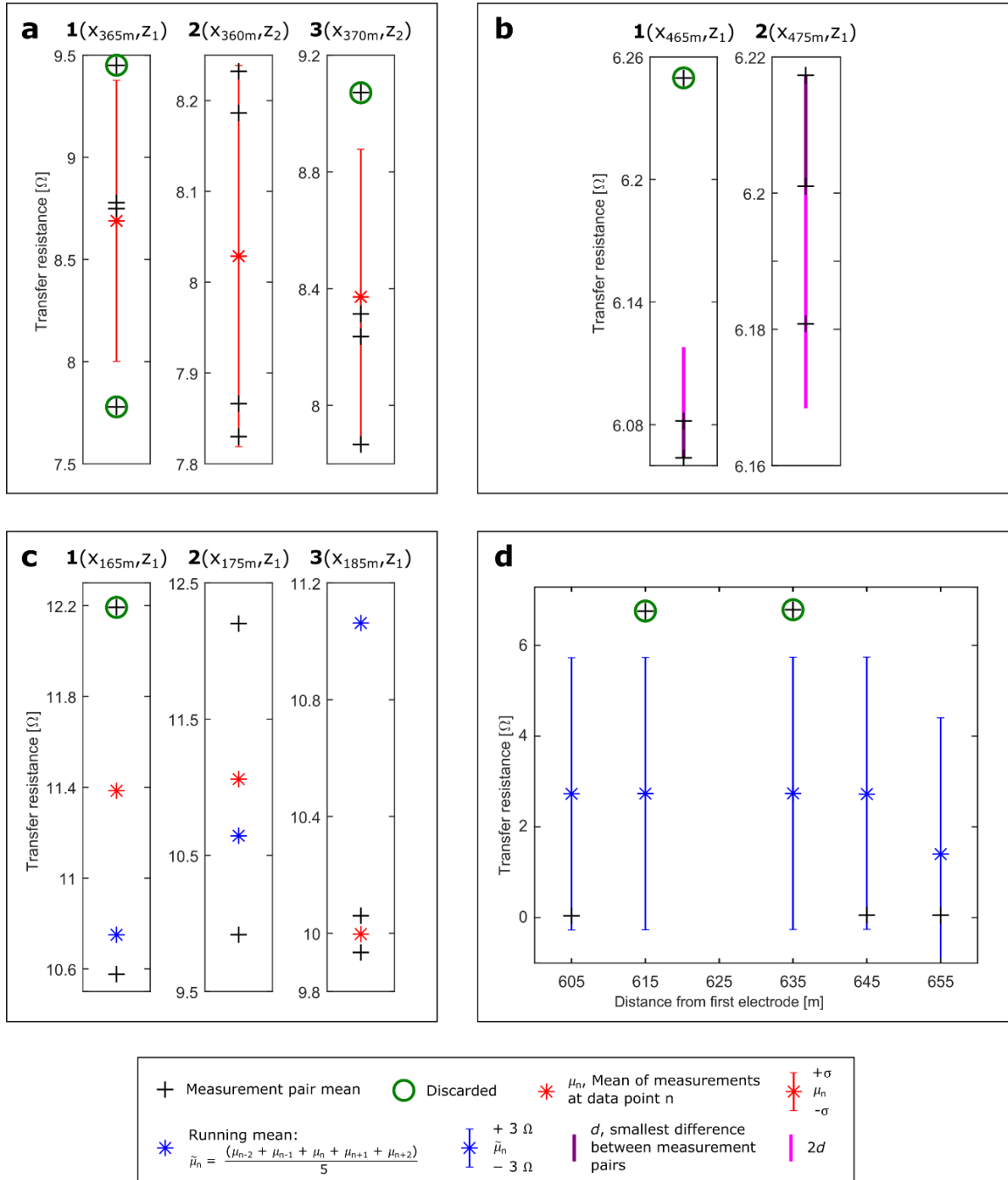
Figure S5. Examples of final data cleaning at data points with four (**a**), three (**b**), two (**c**) and one (**d**) measurements remaining after discarding measurements above the threshold (Figure S3). The examples plotted on panels **a**), **b**), and **c**) are all from Transect A, and the parenthesis on

the subplot labels indicate the data point position on Transect A. The subscripts of x's are defined by the distance to the first electrode in the transect, while the subscript of z's are defined by the relative recording depth. The examples plotted on panel **d**) are all from the shallowest recording depth at Transect D. **a**) When four measurement pairs were available, measurements outside the standard deviation were discarded. As exemplified by subplots 2, 3 and 1, respectively, this procedure implied that zero, one or two measurements were removed. A red line on Figure S2 surrounds these three data points. **b**) At data points with three measurement pairs, the most outlying measurement pair was discarded if the distance to the median was more than twice the distance between the median and the third measurement. Thus, on subplot 1, the uppermost measurement pair was discarded, while on subplot 2, none were. A blue line on Figure S2 surrounds these two data points. **c**) For data cleaning at data points with two measurement pairs, we used a running mean, $\widetilde{\mu}_n$, calculated from the mean, μ_n, of a data point, n, and the four neighboring data points (n-2, n-1, n+1, and n+2). As exemplified by subplot 3, no measurements were discarded when $\widetilde{\mu}_n$ was greater or smaller than both measurement pairs. When $\widetilde{\mu}_n$ was between the measured transfer resistances, the measurement pair with the largest difference to $\widetilde{\mu}_n$ was discarded, but only if the difference between μ_n and $\widetilde{\mu}_n$ was greater than the difference between $\widetilde{\mu}_n$ and the second measurement. This is exemplified by subplot 1, where the measurement pair with the highest transfer resistance was discarded; and by subplot 2, were no measurement was discarded. A green line on Figure S2 surrounds these three data points. **d**) Finally, for data points with only one measurement pair, we discarded it, if the difference to the running mean was greater than 3Ω. A purple line on Figure S2 surrounds the five data points plotted here.
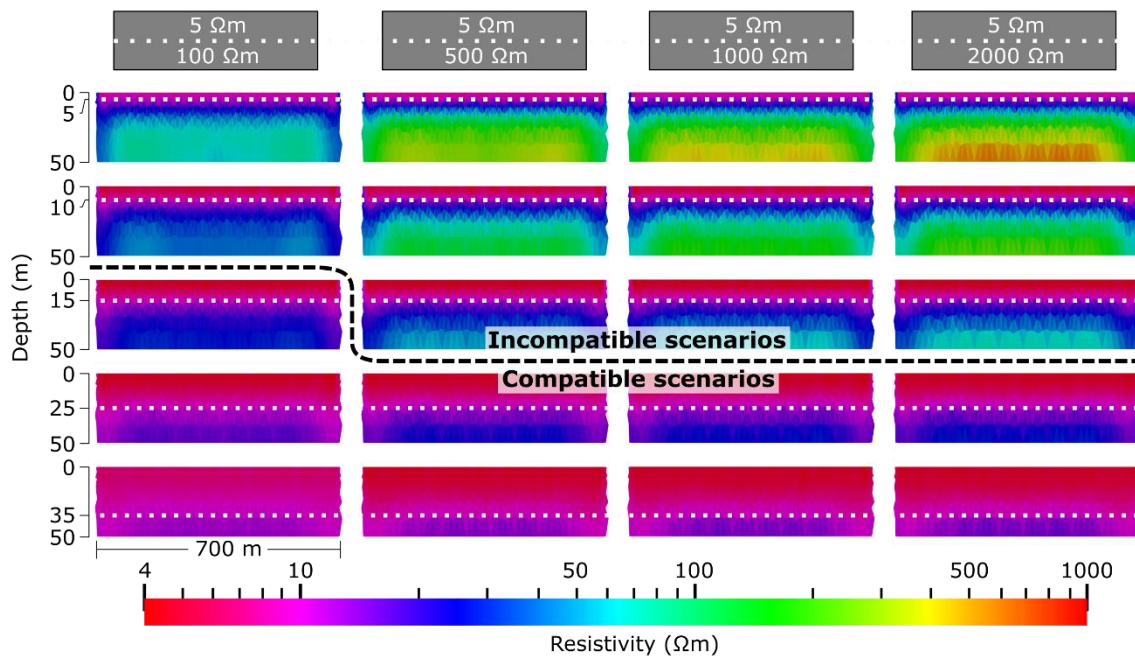
Figure S6. Resistivity models produced by forward modelling experiments intended to reveal the extent to which Segment III (Figure 4) might conceal higher resistivities than the inverted. Scenarios above the black dashed line are incompatible with Segment III, while those below are compatible. The starting models are sketched conceptually at the top of the figure: each consists of two layers, the shallow having a resistivity of 5 Ωm and the deeper a resistivity of

100, 500, 1000 or 2000 Ωm. The depth to the boundary between these two layers is indicated on the vertical axes to the left. The domain, mesh and synthetic measurement protocol was defined so that it mimics setup for the inversion of the field measurements (Section 3).

Table S1 *Summary of measured electrical resistivity data and data cleaning prior to inversion.*

Transect	A	B	C	D
Summary of initial dataset				
Number of surveys in profile	4	3	2	4
Combined length [m]	700	600	500	700
Unique electrode configurations (data point)	605	490	375	605
Number of scheduled measurement pairs	1040	780	520	1040
Not measured / no normal or reciprocal measurement	54	105	31	71
Number of complete measurement pairs	986	675	489	969
… relative to scheduled.	95%	87%	94%	93%
Data points with complete measurement pairs	551	466	344	589
Data coverage	91%	95%	92%	97%
Dataset summary after…				
… removal based on error (normal vs. reciprocal)				
Errors > 5 %	31	13	5	82
Errors > 3σ	19	15	9	16
Number of remaining measurement pairs	*936*	*647*	*475*	*871*
… relative to scheduled	*90%*	*83%*	*91%*	*84%*
Remaining data points				
Data points with one measurement	234	294	197	342
Data points with two measurements	182	127	139	142
Data points with three measurements	94	33		75
Data points with four measurements	14			5
Total number of remaining data points	524	454	336	564
Data coverage	87%	93%	90%	93%
… removal of measurements above transfer resistance threshold				
Threshold (Ω)	20	20	27	20
Measurement pairs above threshold	13	10	11	3
Remaining measurement pairs	923	637	464	868
Data points with one measurement	237	299	202	340
Data points with two measurements	182	121	131	143
Data points with three measurements	90	32		74
Data points with four measurements	13			5
Total number of remaining data points	522	452	333	562
Data coverage	86%	92%	89%	93%
… removal of measurements at data points with four measurement pairs				
Number of remaining measurements	912	637	464	863
Data points with one measurement	237	299	202	340
Data points with two measurements	182	121	131	143
Data points with three measurements	101	32		79
Data points with four measurements	2			0
Total number of remaining data points	522	452	333	562
Data coverage	86%	92%	89%	93%
… removal of measurements at data points with three measurement pairs				

Number of remaining measurements	849	610	464	802
Data points with one measurement	237	299	202	340
Data points with two measurements	245	148	131	204
Data points with three measurements	38	5		18
Data points with four measurements	2			0
Total number of remaining data points	522	452	333	562
Data coverage	86%	92%	89%	93%
… removal of measurements at data points with two measurement pairs				
Number of remaining measurements	806	574	423	768
Data points with one measurement	280	335	243	374
Data points with two measurements	202	112	90	170
Data points with three measurements	38	5		18
Data points with four measurements	2			0
Total number of remaining data points	522	452	333	562
Data coverage	86%	92%	89%	93%
… removal of measurements at data points with one measurement pair				
Number of remaining measurements	*803*	*569*	*418*	*766*
Data points with one measurement	277	330	238	372
Data points with two measurements	202	112	90	170
Data points with three measurements	38	5		18
Data points with four measurements	2			0
Total number of remaining data points	519	447	328	560
Data coverage	86%	91%	87%	93%

Table S1. Summary of measured electrical resistivity data and data cleaning prior to inversion.

Data Set S1. A zipped folder with measured and inverted ERT data from Førstehytte Pingo is public available from the Zenodo repository (Hornum, 2021). The folder has data files containing all measurements and data files with measurements remaining after data cleaning only. The latter were used for the inversion with ResIPy. In addition, inverted resistivity models and electrodes coordinates are also provided. A map of the field site provides a geographical overview. Detailed information about the deposited data files is provided in the readme file.

Movie S1. 3D animation of ERT profiles from FHP pingo. In addition to our own resistivity models, the animation also includes a profile from a survey conducted by Ross et al. (2007). Their profile locates at the crest of FHP.